Vol. 3(Iss. 1) 2026, pp.279-308, African Scientific Annual Review www.asarev.net ISSN: 3007-0902

A Stage-structured population demographic model for organismal development

Olwa Bathlomeo Onyango[1]
Michael Woyengo[2]
George Simmons[3]

olwabathlomeo@gmail.com[1]

[1,2] Department of Pure and Applied Mathematics, Maseno University, Kenya

[3]IDEMS International CIC, United Kingdom

https://doi.org/10.51867/asarev.maths.3.1.23

Abstract

Developmental variability shapes population dynamics, generational turnover, and the timing of ecological processes in stage-structured populations. Distributed Delay Models are the standard tool to capture this variability through compartmental developmental chains, but the intermediate compartments carry no direct biological meaning and their connection to continuous physiological-age dynamics is rarely made explicit. We develop a stage-coupled Kolmogorov Forward Equation framework in which developmental progression is a continuous stochastic process in physiological-age space: advection describes deterministic advancement, diffusion accounts for individual variability, and boundary flux conditions couple successive developmental stages. We show that Distributed Delay Models arise as finite-dimensional approximations of this continuous equation, and derive a moment-based parametrization linking the model coefficients to observed means and variances of developmental duration. Applied to Fall Armyworm (Spodoptera frugiperda) as a case study, the two formulations are compared on their predictions of developmental timing and population peaks to justify the Kolmogorov-based framework as a viable, biologically-motivated alternative to Distributed Delay Models for capturing stage-structured population dynamics.

MSC2010 Subject Classification: Primary 92D25; Secondary 60J60, 35Q92, 65M06
Keywords: Distributed Delay Model, Fall Armyworm, Kolmogorov Forward Equation, Physiological Age, and Stage-Structured Population Dynamics

1 Introduction

Stage-structured population models provide a framework for describing the development of organisms whose life cycles proceed through successive biological stages [6, 15]. A central challenge in such models is representing developmental progression continuously while accounting for variability in the rate at which individuals advance through each stage. Individuals within the same cohort may differ substantially in their developmental durations, resulting in heterogeneous maturation times

Licensed Under Creative Commons Attribution (CC BY-NC)

and overlap between developmental stages [9, 12]. Incorporating this variability within a continuous, stage-structured physiological-age framework therefore remains an important modeling problem.

The McKendrick–von Foerster formulation provides a continuous description of population development in physiological age, but represents developmental progression deterministically [6, 15]. On the other hand, distributed Delay Models (DDMs) address developmental variability by representing a developmental stage as a sequence of compartments connected by transition rates, producing a distributed developmental-time distribution [8, 15]. These models provide a practical representation of heterogeneous developmental durations and have been incorporated widely into physiologically-based demographic models [7, 12] applied to real-world analyses of biological invasion risk, see [**?**]. However, the developmental variability in DDMs is introduced through the compartmental representation rather than through a biological basis in the model itself as compartments generally do not correspond to distinct biological states [6, 8].

This paper develops a stage-structured continuous physiological-age framework based on the Kolmogorov Forward Equation (KFE) for modeling organism development. The formulation represents physiological development within each stage as an advection–diffusion process, in which the advection term describes the mean progression through physiological age and the diffusion term represents variability in developmental progression [3, 6]. The single-stage formulation is extended to a sequence of biological stages through boundary flux conditions that transfer individuals from the terminal boundary of one stage to the initial boundary of the next. This provides a continuous stage-structured formulation in which developmental progression, developmental variability, mortality, and transitions between successive stages are represented within a common framework.

An important consideration is parametrizing population dynamics models against observable population data. By solving the KFE-derived framework in special cases, its parameters are linked to the mean and variance of developmental duration. This provides a moment-based parametrization through which the developmental velocity and diffusion coefficient can be determined from developmental data. A finite-difference scheme is then developed for numerical approximation of the stage-coupled KFE, and its stability, positivity, and monotonicity properties are analysed.

The framework is evaluated in the context of Fall Armyworm (*Spodoptera frugiperda*) as a biological case study. Numerical simulations are used to examine continuous physiological-age distributions, stage transitions, generational turnover, and the effects of developmental velocity, developmental variability, and mortality. The continuous KFE formulation is finally compared with a Distributed Delay Model using corresponding developmental statistics. This comparison is used to examine how the continuous physiological-age formulation and the compartmental formulation represent developmental variability and resulting stage-structured population dynamics.

For the mathematical analysis, we explicitly state the regularity and uniform parabolicity assumptions required for the stochastic and partial differential equation formulations. The coupled stage system is analysed under appropriate compatibility conditions at stage interfaces, while the numerical analysis considers the full stage-coupled system, including boundary fluxes. The relationship between the Distributed Delay Model and the continuous Kolmogorov Forward Equation is examined through the increasing-compartment limit, with the corresponding convergence rate discussed. Mortality effects

Licensed Under Creative Commons Attribution (CC BY-NC)

on developmental-time parametrization are also considered through survival-weighted completion-time distributions. These assumptions and analyses are developed in the subsequent sections.

2 Distributed Delay Models

2.1 Distributed Representation of Development

A fundamental challenge in modeling biological development is the incorporation of developmental variability. Empirical studies consistently show that individuals within the same cohort do not complete development simultaneously, even when subjected to identical environmental conditions [9, 12]. Consequently, developmental models must account not only for the mean developmental duration but also for the variance of development within a cohort. Distributed Delay Models (DDMs) provide a widely used framework for representing such variability in physiologically based demographic models (PBDMs) [7, 8, 15].

In these models, a developmental process is partitioned into a sequence of consecutive sub-stages connected by identical transition rates. Individuals progress sequentially through the sub-stages until completion of development. Consider a developmental cohort divided into k sub-stages. Let $n_i(t)$ denote the population density in sub-stage i, for $i = 1, 2, \ldots, k$. If the mean developmental duration is denoted by Δ, the transition rate between adjacent sub-stages is defined as $r = \frac{k}{\Delta}$. The DDM system is then described by

$$\begin{aligned} \frac{dn_1}{dt} &= -rn_1, \\ \frac{dn_i}{dt} &= r(n_{i-1} - n_i), \qquad i = 2, 3, \ldots, k. \end{aligned} \tag{1}$$

Manetsch [8, p. 548] showed that the compartmental formulation gives rise to a developmental-time distribution of Erlang type, with shape parameter k and rate parameter r. Its density is

$$f_k(t) = \frac{r^k}{(k-1)!} t^{k-1} e^{-rt}, \qquad t \geq 0. \tag{2}$$

The Erlang distribution provides a direct connection between the parameters of the compartmental representation and experimentally observed developmental characteristics. In particular, its mean and variance are

$$\mathbb{E}[T] = \frac{k}{r}, \qquad \mathrm{Var}(T) = \frac{k}{r^2}. \tag{3}$$

The following proposition establishes the parameterization of the DDM in terms of the observed mean developmental duration and variance.

Proposition 2.1. *Let the developmental duration of a cohort be represented by an Erlang distribution with k identical sub-stages and transition rate $r = k/\Delta$. Suppose that the observed mean developmental duration is $u > 0$ and the corresponding variance is $\sigma^2 > 0$. Then the DDM parameters can be chosen*

Licensed Under Creative Commons Attribution (CC BY-NC)

as

$$\Delta = u, \qquad k = \frac{u^2}{\sigma^2}, \qquad r = \frac{u}{\sigma^2}. \tag{4}$$

Moreover, if the corresponding continuous physiological-age model has diffusion coefficient b^2, then matching the variance of the DDM with that of the continuous formulation gives

$$b^2 = \frac{\sigma^2 \Delta^2}{u^3}. \tag{5}$$

Consequently, when $\Delta = u$, the effective diffusion coefficient associated with the k-compartment representation is

$$b^2 = \frac{\Delta}{k}. \tag{6}$$

Proof. From (3), the mean and variance of the developmental-time distribution generated by the DDM are

$$\mathbb{E}[T] = \frac{k}{r}, \qquad \mathrm{Var}(T) = \frac{k}{r^2}.$$

Matching these quantities with the observed mean u and variance σ^2 gives $u = \frac{k}{r}, \qquad \sigma^2 = \frac{k}{r^2}$. Since the total physiological-age interval is taken to be $\Delta = u$, the first relation gives $r = \frac{k}{u}$. Substituting this into the variance relation yields $\sigma^2 = \frac{k}{(\frac{k}{u})^2} = \frac{u^2}{k}$, and hence $k = \frac{u^2}{\sigma^2}$. Therefore, $r = \frac{k}{u} = \frac{u}{\sigma^2}$, which establishes (4).

To relate the compartmental representation to the continuous physiological-age formulation, consider a physiological-age process with mean developmental velocity v and diffusion coefficient b^2. The mean time required to traverse a physiological-age interval of length Δ is $u = \frac{\Delta}{v}$. For the corresponding drift-diffusion process, the variance of the first-passage time is $\sigma^2 = \frac{b^2 \Delta}{v^3}$.

Solving for b^2 gives $b^2 = \frac{\sigma^2 v^3}{\Delta}$. Since $v = \Delta/u$, this can equivalently be written as $b^2 = \frac{\sigma^2 \Delta^2}{u^3}$, which proves (5).
Finally, under the identification $\Delta = u$ and using $\sigma^2 = \frac{u^2}{k}$, we obtain $b^2 = \frac{(u^2/k)u^2}{u^3} = \frac{u}{k} = \frac{\Delta}{k}$. This establishes (6). □

The proposition shows that the diffusion coefficient corresponding to the compartmental representation is $b^2 = \frac{\Delta}{k}$ when the physiological-age interval is normalized so that $\Delta = u$. More generally, without imposing $\Delta = u$, the relationship is $b^2 = \frac{\Delta^2}{uk}$. Thus, for a fixed mean developmental duration and physiological-age interval, the effective diffusion coefficient decreases as the number of compartments k increases.

This relationship should be interpreted as a correspondence between the variability generated by the finite compartmental representation and the diffusion term in the continuous physiological-age formulation. In particular, increasing k while maintaining the same mean developmental duration

Licensed Under Creative Commons Attribution (CC BY-NC)

reduces the variance of the Erlang developmental-time distribution. Consequently, $k \to \infty \implies b^2 \to 0$, and the compartmental model approaches deterministic transport rather than a non-zero-diffusion KFE. Hence, the limiting process obtained by increasing the number of DDM compartments is the deterministic physiological-age transport model, whereas a KFE with $b^2 > 0$ retains developmental variability in the continuous formulation.

2.2 Asymptotic Relation Between the DDM and Continuous Physiological-Age Model

The DDM can be interpreted as a finite-dimensional discretisation of the deterministic physiological-age transport equation. Let the stage interval $[0, \Delta]$ be divided into k uniform compartments of width $\Delta a = \frac{\Delta}{k}$. With developmental velocity $v = \frac{\Delta}{u}$, the transition rate is $r = \frac{v}{\Delta a} = \frac{k}{\Delta} \frac{v}{\Delta} = \frac{k}{u}$. The resulting Erlang completion time has mean u and variance $\frac{u^2}{k}$. Comparing this variance with the first-passage-time variance of the continuous advection-diffusion model gives $b^2 = \frac{\Delta}{k} v = \frac{\Delta^2}{u\,k}$
Thus, each finite value of k corresponds to a continuous diffusion model with diffusion coefficient $b^2 = \frac{\Delta^2}{u\,k}$. As k increases, b^2 decreases and the developmental-time variance tends to zero. Consequently, for fixed mean developmental duration, the k-compartment DDM approaches deterministic physiological-age transport as $k \to \infty$. This establishes the precise relationship between the compartment number and the effective diffusion coefficient. The DDM therefore provides a finite-dimensional approximation to physiological-age transport, while the KFE introduces developmental variability directly through the diffusion term. The two formulations should consequently be compared at matched developmental means and variances rather than identifying the limit $k \to \infty$ with a non-zero diffusion KFE.

2.3 Limitations of Distributed Delay Models

Despite their widespread use, DDMs have several limitations. Increasing the number of compartments increases the dimension of the system and may therefore increase computational cost, particularly for complex life cycles [7, 12]. Moreover, the intermediate compartments do not generally correspond to observable biological states; rather, they are introduced to generate a desired developmental-time distribution. Consequently, developmental variability is represented indirectly through the compartmental structure, making its biological interpretation less direct. We explore this gap more concretely in Section 3.1.The correspondence derived above also clarifies that increasing the number of DDM compartments does not by itself produce a continuous model with fixed non-zero developmental diffusion. Rather, under fixed mean developmental duration, the effective diffusion coefficient decreases as $\frac{1}{k}$. The continuous KFE considered in this study therefore represents a distinct stochastic formulation whose diffusion coefficient is calibrated independently from observed developmental variability.

Licensed Under Creative Commons Attribution (CC BY-NC)

3 A stage-structured Kolmogorov Forward Equation Framework

Demographic population models accounting for physiological age stem from the McKendrick-von Forester partial differential equation. In its simplest form, this is given by

$$\frac{\partial n}{\partial t} = -\frac{\partial n}{\partial a}, \tag{7}$$

where $n(t, a)$ is population density and a is the physiological age of the population.

3.1 DDM – McKendick-von Foerster comparison

The McKendick-von Foerster equation (7) propagates an initial population distribution $n(0, a) = n_0(a)$ as

$$n(t, a) = n_0(a - t).$$

In particular, no developmental variability can be accounted for by this model. On the other hand, the DDM system can be viewed as a certain discretisation of (7), as follows.

Proposition 3.1. *Partition the physiological age domain $a = [0, \Delta]$ into k uniform compartments of width $\Delta a = \frac{\Delta}{k}$. Then approximating the right-hand side of (7) with backwards finite difference coincides with system (1).*

Proof. Let $n_i(t) \approx n(t, a_i)$, where $a_i = i\,\Delta a$. Replacing the spatial derivative by the backward upwind difference gives,

$$\frac{dn_i}{dt} = -\frac{n_i - n_{i-1}}{\Delta a} = \frac{k}{\Delta}\left(n_{i-1} - n_i\right) \tag{8}$$

Setting $r = \frac{k}{\Delta}$ in (8) recovers the system (1). Therefore, the DDM is a backward finite difference discretization of (7) in physiological age. □

The DDM can therefore be interpreted as a finite-dimensional discretization of the deterministic physiological-age transport equation. The variability in developmental completion times observed in the DDM arises from the sequential compartmental transition structure and the resulting distribution of transit times across the compartments. Thus, the variability is induced by the compartmental representation rather than introduced as an explicit stochastic diffusion process in the underlying physiological-age dynamics. In contrast, the KFE incorporates developmental variability directly through the diffusion term, allowing the magnitude of this variability to be specified independently of the physiological-age discretization.

Licensed Under Creative Commons Attribution (CC BY-NC)

3.2 Single-stage dynamics Equation

Proposition 3.2. *Let A_t denote the continuous physiological age of an individual within stage s. The age progression of the individul is modeled via the stochastic differential equation(SDE)*

$$dA_t = v_s(t, A_t)\, dt + b_s(t, A_t)\, dW_t$$

To guarantee existence and uniqueness of a strong solution to the stochastic differential equation. Assume that for each stage s, the coefficients $v_s(t, a)$ and $b_s(t, a)$ are continuous in (t, a), globally Lipschitz in a uniformly in t, and satisfy the linear growth condition

$$|v_s(t, a)| + |b_s(t, a)| \leq K(1 + |a|),$$

for some constant $K > 0$. For the associated KFE, we additionally assume that v_s and b_s^2 are continuously differentiable in a and that the diffusion is uniformly positive, there exists $b_{0,s}^2 > 0$ such that $b_s^2(t, a) \geq b_{0,s}^2$, $\forall\ (t, a) \in [0, T] \times [0, \Delta_s]$. These conditions ensure that the equation is uniformly parabolic and allow the standard weak-solution theory for linear parabolic equations to be applied.

Proof. Applying the Itô's formula to any arbitrary test function $\phi \in C_c^\infty([0, \Delta_s])$ yields [10]

$$d\phi(A_t) = \left[v_s(t, A_t)\, \phi'(A_t) + \frac{1}{2} b_s^2(t, A_t)\, \phi''(A_t) \right] dt + b_s(t, A_t)\, \phi'(A_t)\, dW_t$$

Taking expectations having $\mathcal{E}\left[dW_t\right] = 0$ and integrating by part against the stage density $n_s(t, a)$ over the domain $[0, \Delta_s]$ recovers the governing KFE [3, 6]

$$\boxed{\frac{\partial n_s(t, a)}{\partial t} \;=\; -\frac{\partial}{\partial a}\ \left(v_s(t, a)\ n_s(t, a)\right) \;+\; \frac{1}{2}\ \frac{\partial^2}{\partial a^2}\ \left(b_s^2(t, a)\ n_s(t, a)\right) \;-\; \mu_s(t, a)\ n_s(t, a),} \tag{9}$$

Mortality is incorporated as a killing term. □

The case $b_s^2 = 0$ is excluded from the parabolic analysis above. In this limiting case, the KFE reduces to a first-order transport equation of McKendrick–von Foerster type and requires a different boundary treatment. The present analysis therefore assumes uniformly positive diffusion within each developmental stage.
The conservative physiological-age flux is defined by

$$J_s(t, a) = v_s(t, a)\ n_s(t, a) - \frac{1}{2}\ \partial a\ \left(b_s^2(t, a)\ n_s(t, a)\right) \tag{10}$$

Expanding the derivative gives

$$J_s(t, a) = \left[v_s(t, a) - \frac{1}{2}\ \partial a\ b_s^2(t, a) \right]\ n_s(t, a) - \frac{1}{2}\ b_s^2(t, a)\ \partial a\ n_s(t, a)$$

Thus, when the diffusion coefficient varies with physiological age, its spatial derivative contributes an

Licensed Under Creative Commons Attribution (CC BY-NC)

additional effective drift term. When b_s^2 is constant within a stage, this derivative vanishes and the flux reduces to

$$J_s(t,a) = v_s\, n_s(t,a) - \frac{1}{2}\, b_s^2\, \partial a\, n_s(t,a)$$

The conservative form is used below so that the stage equations remain consistent with the underlying KFE for both constant and variable diffusion coefficients.

3.3 Continuous Physiological Age and Stage Structured Population Dynamics

The modified KFE framework (9) of Bellagamba and Di Cola gives a model continuous in physiological age in which developmental variability can be controlled explicitly. It does not, however, account for sequential progression of individuals through multiple developmental stages.

We extend this framework to a stage-structured formulation. We assume that completion of one stage generates recruitment into the subsequent stage, creating a system of population flows. Consider a population whose life cycle consists of n consecutive developmental stages, $S = \{s_1, s_2, \ldots, s_n\}$. A developmental stage $s \in S$ occupies a physiological age domain $a \in [0, \Delta_s]$. The quantity Δ_s denotes the physiological age threshold corresponding to completion of stage s. Individuals enter a stage at physiological age $a = 0$ and progress continuously until reaching $a = \Delta_s$, at which point they transition into the subsequent stage, except for individuals completing the final stage s_n, who leave the population.

3.4 Stage Coupling Through Boundary Fluxes

The KFE for each developmental stage can be written in conservative form as

$$\frac{\partial n_s(t,a)}{\partial t} \;=\; -\,\frac{\partial J_s(t,a)}{\partial a} \;-\; \mu_s(t,a)\, n_s(t,a), \tag{11}$$

where the physiological age flux is (10)
Consider a life cycle consisting of consecutive stages $s_1, \ldots, s_n$. We assume that stage transitions are instantaneous and that individuals leaving stage s_i enter stage s_{i+1} without additional loss at the transition boundary. Hence, the transition is imposed through equality of the outgoing and incoming population fluxes

$$J_{s_{i+1}}\,(t,0) \;=\; J_{s_i}\,(t,\Delta_{s_i}), \quad i \;=\; 1,2,\ldots,n-1. \tag{12}$$

The equality of fluxes in (12), rather than equality of boundary densities, is the appropriate interface condition because individuals are transferred between biological stages through population flow. The condition is imposed together with the regularity assumptions on v_s, b_s^2 and μ_s stated in Section 3.2 and the initial compatibility condition stated above.
For the first stage, recruitment is generated by reproduction from the terminal stage. Let $\beta_n(t,a)$ denote the reproduction rate of individuals in the final stage s_n. The recruitment flux is given by

$$J_{s_1}(t,0) = R(t) = \int_0^{\Delta_{s_n}} \beta(t,a)\, n_{s_n}(t,a)\, da. \tag{13}$$

Licensed Under Creative Commons Attribution (CC BY-NC)

We assume that the reproduction functional $R(t)$ is well defined and locally Lipschitz with respect to the terminal-stage density n_{s_n}. Under these assumptions, the reproductive boundary condition defines a well-posed inflow into the first developmental stage.

These boundary conditions couple the individual stage equations into a complete stage-structured population model. Consequently, for each stage $s \in S$, the population density satisfies (11),subject to the stage-transition conditions (12) and the recruitment condition (13). This formulation provides a continuous physiological-age description of the complete life cycle, with developmental stages coupled through population fluxes at their boundaries.

Theorem 3.1 (Well-Posedness of the Stage-Coupled System)**.** *Assume, for every stage s, that v_s and b_s^2 are continuously differentiable in (t,a), μ_s is continuous, and there exists $b_{0,s}^2 > 0$ such that $b_s^2(t,a) \geq b_{0,s}^2$. Let the initial densities satisfy $n_{s,0} \in L^2(0,\Delta_s)$, and assume compatibility of the initial data with the stage-interface and reproductive boundary fluxes. Suppose also that the recruitment functional $R(t)$ is locally Lipschitz with respect to the terminal-stage density.*

Then the stage-coupled system (11) - (13) *admits a unique weak solution satisfying*

$$n_s \in L^2(0,T;H^1(0,\Delta_s)) \cap C([0,T];L^2(0,\Delta_s)),$$

for each developmental stage s.

Proof. The result follows from the standard weak formulation of linear uniformly parabolic equations. For each stage, the uniform lower bound on b_s^2 provides coercivity of the diffusion operator. A Galerkin approximation is constructed in a finite-dimensional subspace of $H^1(0,\Delta_s)$. Testing the resulting equations with the corresponding approximate solution and summing over all stages gives an energy estimate [10]. At the internal interfaces between successive stages, the boundary contributions occur with opposite orientations. The flux-continuity condition $J_{s_i}(t,\Delta_{s_i}) = J_{s_{i+1}}(t,0)$ therefore ensures that the corresponding internal boundary contributions cancel when the energy identities for adjacent stages are summed.

The reproductive boundary at $a = 0$ of the first stage is different, since it is an external boundary and does not have an adjacent stage with which its contribution can cancel. Its contribution is determined by $J_{s_1}(t,0) = R(t)$, where $R(t) = \int_0^{\Delta_{s_n}} \beta(t,a) n_{s_n}(t,a)\, da$. Under the assumed local Lipschitz and regularity properties of the recruitment functional, this boundary contribution can be bounded in terms of the stage densities. Consequently, the summed energy estimate takes the form

$$\frac{d}{dt}\sum_{s\in S}\|n_s(t,\cdot)\|^2_{L^2(0,\Delta_s)} + C_1\sum_{s\in S}\|n_s(t,\cdot)\|^2_{H^1(0,\Delta_s)} \leq C_2\sum_{s\in S}\|n_s(t,\cdot)\|^2_{L^2(0,\Delta_s)},$$

for suitable constants $C_1 > 0$ and $C_2 \geq 0$, after applying the trace inequality and the assumed bound on the recruitment functional. Grönwall's inequality then gives a uniform bound in $L^\infty(0,T;L^2) \cap L^2(0,T;H^1)$. Weak compactness yields existence of a weak solution, while applying the same energy estimate to the difference of two solutions gives uniqueness. □

Example 3.1. *To illustrate, consider a two-stage insect system consisting of an egg stage s_1 and an adult stage s_2. Individuals enter the egg stage at $a = 0$ with prescribed inflow $J_{s_1}(t,0) = R(t)$,*

Licensed Under Creative Commons Attribution (CC BY-NC)

representing adult reproduction. As eggs complete development at $a = \Delta_{s_1}$, the outflow is $J_{s_1}(t, \Delta_{s_1})$ representing hatching and immediately constitutes the adult recruitment flux $J_{s_2}(t, 0)$. This coupling mechanism extends naturally to any finite number of developmental stages providing a continuous physiological age description of a complete life cycle.

3.5 Improvement over existing methods

The KFE framework possesses several advantages over traditional compartmental formulations. First, physiological age is represented as a continuous variable, eliminating the need for artificial developmental compartments. Second, developmental variability is incorporated explicitly through the diffusion term, providing a direct biological interpretation of stochastic developmental processes. Third, stage coupling i achieved through physiologically meaningful boundary fluxes that preserve conservation of population. Finally, the framework accommodates arbitrary life-cycle structures and therefore remains applicable to a wide range of stage-structured organisms.
Having established the continuous stage-structured formulation, the next section develops analytical solutions and parametrization methods that connect the model coefficients to experimentally observed developmental durations.

4 Analytical Parametrization of the KFE framework

Consider a single developmental stage $s \in S$ with physiological-age domain $a \in [0, \Delta_s]$. To establish a direct relationship between the KFE coefficients and observable developmental characteristics, assume that the developmental velocity and diffusion coefficient are constant within the stage, so that

$$v_s(t, a) \;=\; v_s, b_s^2(t, a) \;=\; b_s^2,$$

with $v_s > 0$ and $b_s^2 > 0$. An individual entering stage s is assumed to have initial physiological age $A_0 = 0$. For the purpose of deriving the developmental completion-time distribution, mortality is temporarily neglected, so that $\mu_s = 0$. The governing equation then becomes

$$\frac{\partial n_s}{\partial t} \;=\; -v_s \frac{\partial n_s}{\partial a} \;+\; \frac{b_s^2}{2} \frac{\partial^2 n_s}{\partial a^2}.$$

This equation corresponds to the forward equation associated with the stochastic physiological-age process

$$dA_t \;=\; v_s \, dt + b_s \, dW_t,$$

where W_t denotes a standard Brownian motion. Stage completion occurs when physiological age first reaches the terminal threshold Δ_s. Define the first-passage time by

$$\tau_s = \inf \{t > 0 : A_t \geq \Delta_s\}.$$

The boundary $a = \Delta_s$ is therefore interpreted as an absorbing completion boundary for the single-stage first-passage problem. Once an individual reaches Δ_s, it leaves the current developmental

Licensed Under Creative Commons Attribution (CC BY-NC)

stage. In the full stage-structured model, the corresponding outgoing flux is transferred to the next developmental stage through the boundary coupling defined in Section 3. Thus, τ_s represents the time required for an individual entering stage s at physiological age zero to complete that developmental stage.

For the analytical derivation below, we assume that individuals enter stage s at physiological age $A_0 = 0$ and that the stage-completion boundary $a = \Delta_s$ is absorbing. Mortality is initially set to zero so that the intrinsic developmental-time distribution can be derived independently of survival. The effect of mortality on the observed completion-time distribution is considered separately in Section 4.2.1.

4.1 Developmental Completion Times

Consider a single developmental stage $s \in S$ with physiological-age domain $a \in [0, \Delta_s]$. To establish a direct relationship between the KFE coefficients and observable developmental characteristics, assume that the developmental velocity and diffusion coefficients are constant within the stage, so that

$$v_s(t, a) = v_s, \qquad b_s^2(t, a) = b_s^2.$$

For the purpose of deriving developmental completion times, mortality is temporarily neglected. The governing equation then becomes

$$\frac{\partial n_s}{\partial t} = -v_s \frac{\partial n_s}{\partial a} + \frac{b_s^2}{2} \frac{\partial^2 n_s}{\partial a^2}, \tag{14}$$

For the first-passage-time problem, the terminal boundary is absorbing, so that $n_s(t, \Delta_s) = 0$. This condition represents completion of the developmental stage: individuals reaching $a = \Delta_s$ leave the current stage and their outgoing flux is transferred to the next stage through the coupling condition in Section 3.4.

Equation (14) corresponds to the forward equation associated with the stochastic physiological-age process

$$dA_t = v_s \, dt + b_s \, dW_t, \tag{15}$$

where W_t denotes a standard Brownian motion. The developmental completion time is therefore represented by the first-passage time at which physiological age reaches the terminal value Δ_s. Define

$$\tau_s = \inf\{t > 0 : A_t = \Delta_s\}. \tag{16}$$

Thus, τ_s represents the time required for an individual to complete developmental stage s.

4.2 First-Passage-Time Distribution and Parameter Estimation

A standard result for a Brownian motion with positive drift states that the first-passage time to a fixed positive threshold follows an inverse Gaussian distribution [13, 14]. Applying this result to the process (15), with threshold Δ_s, gives the following result.

Proposition 4.1. *Consider the stochastic physiological-age process $dA_t = v_s \, dt + b_s \, dW_t$, with $v_s > 0$ and $b_s^2 > 0$, initialized at $A_0 = 0$. Let the developmental stage be completed when the process first*

Licensed Under Creative Commons Attribution (CC BY-NC)

reaches the absorbing threshold $\Delta_s > 0$. *Then the completion time* $\tau_s = inf t > 0 : A_t = \Delta_s$ *follows an inverse Gaussian distribution* $IG(u_s, \lambda_s)$, *with density function:*

$$f_s(t) = \sqrt{\frac{\lambda_s}{2\pi t^3}} \exp\left(-\frac{\lambda_s (t-u_s)^2}{2u_s^2 t}\right), \quad t > 0 \tag{17}$$

where the mean developmental duration u_s *and shape parameter* λ_s *are related to the advection velocity* v_s *and diffusion coefficient* b_s^2 *by:*

$$u_s = \frac{\Delta_s}{v_s}, \quad \lambda_s = \frac{\Delta_s^2}{b_s^2} \tag{18}$$

Proof. For the stochastic process

$$A_t = v_s\, t + b_s\, W_t,$$

the first-passage time to the level $\Delta_s > 0$ has an inverse Gaussian distribution. In the standard parametrization, the mean parameter is given by the threshold divided by the drift,

$$u_s = \frac{\Delta_s}{v_s},$$

while the shape parameter is

$$\lambda_s = \frac{\Delta_s^2}{b_s^2}.$$

Substitution of these parameters into the standard inverse Gaussian density gives (17). □

The inverse Gaussian distribution has mean and variance

$$\mathbb{E}[\tau_s] = u_s, \qquad \mathrm{Var}(\tau_s) = \frac{u_s^3}{\lambda_s}.$$

Using (18), the mean developmental duration is therefore

$$u_s = \frac{\Delta_s}{v_s}, \tag{19}$$

while its variance is

$$\sigma_s^2 = \frac{b_s^2 \Delta_s}{v_s^3}. \tag{20}$$

These expressions establish the connection between the KFE framework coefficients and experimentally observable developmental statistics. If the mean developmental duration u_s and variance σ_s^2 are available from biological observations, the model coefficients can be obtained by rearranging (19)

Licensed Under Creative Commons Attribution (CC BY-NC)

and (20):

$$\begin{aligned} v_s &= \frac{\Delta_s}{u_s}, \\ b_s^2 &= \frac{\sigma_s^2 \Delta_s^2}{u_s^3}. \end{aligned} \tag{21}$$

4.2.1 Parameter Estimation in the Presence of Mortality

The mortality-free parametrization in Section 4.2 identifies v_s and b_s^2 from the intrinsic mean and variance of developmental completion time. When mortality is present, however, developmental observations from surviving individuals are subject to survival selection. The observed completion-time density is therefore not the intrinsic first-passage density but the survival-weighted density

$$f_s^{obs}(t) = \frac{f_s(t)e^{-\mu_s t}}{\int_0^\infty f_s(\xi)e^{-\mu_s \xi} d\xi}$$

Consequently, the observed mean and variance generally differ from the intrinsic developmental moments. If μ_s is known independently, the mortality-adjusted moments can be used to recover the intrinsic parameters v_s and b_s^2. If μ_s is unknown, the two observed moments alone are insufficient to identify the three parameters (v_s, b_s^2, μ_s). In that case, mortality must either be estimated independently from survival data or additional observations must be incorporated into the parameter-estimation procedure.

Evaluating the moment-generating function of the Inverse Gaussian distribution under this mortality weighting yields the observed mean $u_s^{obs} = \mathbb{E}[\tau_s \mid \text{survival}]$ and observed variance $(\sigma_s^2)^{obs} = \text{Var}(\tau_s \mid \text{survival})$:

$$u_s^{obs} = \frac{u_s}{\sqrt{1 + \frac{2\mu_s u_s^2}{\lambda_s}}} = u_s \left(1 - \frac{\mu_s \sigma_s^2}{u_s} + \mathcal{O}(\mu_s^2)\right)$$

$$(\sigma_s^2)^{obs} = \frac{\sigma_s^2}{\left(1 + \frac{2\mu_s u_s^2}{\lambda_s}\right)^{3/2}} = \sigma_s^2 \left(1 - \frac{3\mu_s \sigma_s^2}{2u_s} + \mathcal{O}(\mu_s^2)\right)$$

Bias-Corrected Estimators:To prevent systemic underestimation of intrinsic developmental variance in high-mortality environments, empirical cohort data $(u_s^{obs}, (\sigma_s^2)^{obs})$ must be corrected prior to parameterizing the KFE. Inverting the first-order perturbation expansions yields the intrinsic cohort moments:

$$u_s \approx u_s^{obs} \left(1 + \frac{\mu_s (\sigma_s^2)^{obs}}{u_s^{obs}}\right)$$

$$\sigma_s^2 \approx (\sigma_s^2)^{obs} \left(1 + \frac{3\mu_s (\sigma_s^2)^{obs}}{2u_s^{obs}}\right)$$

Licensed Under Creative Commons Attribution (CC BY-NC)

The intrinsic advection velocity v_s and diffusion coefficient b_s^2 are then parameterized directly using the corrected moments (21). For constant mortality μ_s, the survival-weighted completion density can be normalized using the Laplace transform of the inverse Gaussian distribution. The resulting conditional moments describe the developmental durations among individuals that survive to completion.

4.3 Relationship with Distributed Delay Models

Distributed Delay Models (DDMs) and the KFE framework provide two different representations of developmental variability. In a DDM, a developmental stage is represented by a sequence of k_s compartments connected by transition rates [6, 8]. The resulting developmental completion time follows an Erlang distribution, with its mean and variance determined by the compartment transition parameters (4).

For the KFE, developmental progression is represented continuously in physiological-age space. The mean rate of progression is controlled by the developmental velocity v_s, while developmental variability is controlled independently through the diffusion coefficient b_s^2 [3, 6].

The parametrization in (21) therefore provides a direct link between experimentally observed developmental statistics and the KFE coefficients. In particular, the mean developmental duration determines v_s, while the observed variance determines the magnitude of b_s^2. This allows the KFE and DDM to be compared using equivalent developmental means and variances while retaining their distinct representations of developmental progression. This is the subject of Section 6.7.

The resulting parametrization provides the basis for the numerical experiments in the following sections, where the KFE coefficients are specified from developmental characteristics and the resulting population dynamics are compared with those generated by the corresponding DDM.
When mortality is present, the comparison between the KFE and DDM should be based on the same mortality rate as well as matched intrinsic developmental moments. Matching only the observed mean and variance of surviving individuals can produce different intrinsic parameter values because mortality selectively removes slower-developing individuals. Therefore, in the numerical comparison below, mortality is treated as a separate demographic parameter and the developmental parameters are obtained from the intrinsic developmental statistics.

5 Numerical Discretisation and Stability Analysis

The analytical parametrization developed in the previous section provides a direct relationship between the KFE coefficients and observable developmental statistics. The resulting stage-coupled KFE, however, does not generally possess a closed-form solution for the complete life-cycle system. This remains the case even when the developmental coefficients are constant within each stage, because the coupling conditions at the stage boundaries introduce time-dependent inflow conditions determined by the population flux from neighbouring stages. Numerical discretisation is therefore required to approximate the solution of the coupled system.

Licensed Under Creative Commons Attribution (CC BY-NC)

5.1 Finite Difference Approximation

We discretize the physiological age domain $[0, \Delta_s]$ into N_a uniform intervals of width $\Delta a = \frac{\Delta_s}{N_a}$. Let $a_i = i\Delta a$, $i = 0, 1, \ldots, N_a$, and let $t_j = j\Delta t$. We denote the numerical approximation to $n_s(t_j, a_i)$ by $n_{s,i}^j$.

Using the conservative form of the KFE,

$$\frac{\partial n_s}{\partial t} = -\frac{\partial J_s}{\partial a} - \mu_s n_s,$$

with $J_s = v_s n_s - \frac{1}{2} b_s^2 \frac{\partial n_s}{\partial a}$, we employ a backward-Euler discretization in time and a first-order upwind approximation for the advective flux together with a centered approximation for the diffusive flux. For constant v_s, b_s^2, and μ_s within a stage, the resulting interior scheme is

$$\frac{n_{s,i}^{j+1} - n_{s,i}^j}{\Delta t} = -v_s \frac{n_{s,i}^{j+1} - n_{s,i-1}^{j+1}}{\Delta a} + \frac{b_s^2}{2} \frac{n_{s,i+1}^{j+1} - 2n_{s,i}^{j+1} + n_{s,i-1}^{j+1}}{(\Delta a)^2} - \mu_s n_{s,i}^{j+1}.$$

Define the dimensionless quantities

$$C_s = \frac{v_s \Delta t}{\Delta a}, \qquad D_s = \frac{b_s^2 \Delta t}{2(\Delta a)^2}, \qquad G_s = \mu_s \Delta t.$$

Then the interior scheme can be written as

$$-(C_s + D_s) n_{s,i-1}^{j+1} + (1 + C_s + 2D_s + G_s) n_{s,i}^{j+1} - D_s n_{s,i+1}^{j+1} = n_{s,i}^j, \quad i = 1, \ldots, N_a - 1. \tag{22}$$

The backward-Euler discretization is first-order accurate in time, while the upwind and centered spatial approximations are first-order and second-order accurate, respectively. Consequently, the local truncation error of the combined interior scheme is $\mathcal{O}(\Delta t + \Delta a)$.
The upwind approximation introduces numerical diffusion in addition to the physical diffusion represented by $b_s^2/2$. For the first-order upwind discretization, the leading artificial-diffusion coefficient associated with the advective term is

$$D_{\text{num}} = \frac{v_s \Delta a}{2}.$$

To ensure that this artificial diffusion remains small relative to the physical diffusion, it is desirable to impose $D_{\text{num}} \ll \frac{b_s^2}{2}$,or equivalently, $v_s \Delta a \ll b_s^2$. This requirement can be expressed through the cell Peclet number $Pe_{\text{cell}} = \frac{v_s \Delta a}{b_s^2}$. Thus, $Pe_{\text{cell}} \ll 1$ ensures that numerical diffusion introduced by the upwind approximation remains small relative to the physical developmental diffusion. This is a spatial-resolution condition rather than a stability restriction on the time step. Because the present scheme uses backward Euler in time, no CFL restriction on Δt is required for stability of the interior discretization.

The fully implicit backward-Euler scheme is therefore preferable for the present stage-coupled problem, particularly when fine physiological-age meshes are required. At each time step, the interior equations

Licensed Under Creative Commons Attribution (CC BY-NC)

together with the stage-interface and reproductive boundary conditions form a global linear system $A\mathbf{n}^{j+1} = \mathbf{n}^j$, where $\mathbf{n}^j$ contains the population densities at all physiological-age nodes and across all developmental stages. The interface conditions are incorporated directly into A, so the stability and positivity properties of the complete numerical scheme must be established for this global system rather than for the interior discretization alone.

5.2 Discrete Stage-Coupling Boundary Conditions

The coupling between developmental stages must be imposed through physiological-age fluxes rather than through direct equality of boundary densities. Let $J_s(t,a) = v_s n_s(t,a) - \frac{b_s^2}{2}\frac{\partial n_s}{\partial a}$, where the coefficients are assumed constant within stage s.

For the interface between stages s and $s+1$, the continuous coupling condition is $J_{s+1}(t,0) = J_s(t,\Delta_s)$. At the terminal boundary $a = \Delta_s$, approximate the outgoing flux by:

$$J_s(t,\Delta_s) \approx v_s n_{s,N_a} - \frac{b_s^2}{2\Delta a}\left(n_{s,N_a} - n_{s,N_a-1}\right).$$

Similarly, the incoming flux to stage $s+1$ is approximated by:

$$J_{s+1}(t,0) \approx v_{s+1} n_{s+1,0} - \frac{b_{s+1}^2}{2\Delta a}\left(n_{s+1,1} - n_{s+1,0}\right).$$

Consequently, the numerical stage-coupling condition is obtained by:

$$v_{s+1} n_{s+1,0}^{j+1} - \frac{b_{s+1}^2}{2\Delta a}\left(n_{s+1,1}^{j+1} - n_{s+1,0}^{j+1}\right) = v_s n_{s,N_a}^{j+1} - \frac{b_s^2}{2\Delta a}\left(n_{s,N_a}^{j+1} - n_{s,N_a-1}^{j+1}\right). \tag{23}$$

The interface equations are included directly in the global linear system and are therefore part of the stability and positivity analysis. In particular, stability of the interior finite-difference operator alone is not sufficient to establish stability of the complete stage-coupled scheme. The boundary coupling coefficients must also satisfy the sign and diagonal-dominance conditions required for the global coefficient matrix to be an M-matrix.
At an interface between stages s and $s+1$, the discrete flux condition produces off-diagonal coupling terms between the terminal node of stage s and the initial node of stage $s+1$. These terms are retained explicitly in the global block system rather than being treated as independent boundary data. The resulting matrix therefore has the block-tridiagonal structure associated with the sequential stage coupling.

For the first developmental stage, reproduction provides the incoming flux. If $R(t) = \int_0^{\Delta_{sn}} \beta(t,a) n_{s_n}(t,a)\, da$, then the numerical boundary condition is $J_{s_1}(t,0) = R(t)$. This formulation ensures that both stage transitions and reproduction are represented as population fluxes, consistent with the continuous stage-coupled KFE.

Licensed Under Creative Commons Attribution (CC BY-NC)

5.3 Stability, Positivity, and Monotonicity

We first state the numerical properties considered in this section. The numerical scheme is said to be stable if the numerical solution remains bounded for bounded initial and boundary data. For the interior discretization, unconditional ℓ^2-stability is established by the von Neumann analysis below. The scheme is positivity preserving if $n_{s,i}^j \geq 0$ for all stages, spatial nodes, and time levels whenever the initial data and prescribed boundary inflows are non-negative. A matrix A is an M-matrix if it is a Z-matrix, that is, all its off-diagonal entries are non-positive, and $A^{-1} \geq 0$ componentwise. The scheme is monotone if, for two numerical solutions with identical non-negative boundary data, $\mathbf{n}^j \leq \mathbf{m}^j$ implies $\mathbf{n}^{j+1} \leq \mathbf{m}^{j+1}$.

Theorem 5.1 (Conditional Positivity and Monotonicity of the Fully Implicit Scheme)**.** *Consider the fully implicit finite-difference approximation of the stage-coupled KFE defined by the interior scheme* (22) *together with the discrete flux-coupling conditions in Section 5.2. Assume, for every stage* s, $v_s > 0, \quad b_s^2 \geq 0, \quad \mu_s \geq 0$, *and suppose that the discrete boundary and interface equations are incorporated into the global coefficient matrix* A*. If* A *is a nonsingular* M*-matrix, then the fully implicit scheme is positivity preserving and monotone. Moreover, the interior discretization is unconditionally stable in the* ℓ^2 *sense.*

Proof. We first establish stability of the interior discretization. Consider a Fourier mode $n_{s,i}^j = \zeta^j e^{\mathrm{i}i\theta}$, where θ is the spatial wave number. Substitution into (22) gives

$$\zeta = \frac{1}{1 + C_s(1 - e^{-\mathrm{i}\theta}) + 2D_s(1 - \cos\theta) + G_s}.$$

Let $A_s(\theta) = C_s(1 - e^{-\mathrm{i}\theta}) + 2D_s(1 - \cos\theta) + G_s$. Since $C_s \geq 0, \quad D_s \geq 0, \quad G_s \geq 0$, we have

$$\operatorname{Re} A_s(\theta) = C_s(1 - \cos\theta) + 2D_s(1 - \cos\theta) + G_s \geq 0.$$

Consequently,

$$|1 + A_s(\theta)|^2 = (1 + \operatorname{Re} A_s(\theta))^2 + (\operatorname{Im} A_s(\theta))^2 \geq 1.$$

Therefore,

$$|\zeta| = \frac{1}{|1 + A_s(\theta)|} \leq 1.$$

Hence the interior discretization is unconditionally stable in the ℓ^2 sense for all $\Delta t > 0, \quad \Delta a > 0$. This von Neumann argument applies only to the interior equations. The stage-interface and reproductive boundary conditions are not represented by a translation-invariant operator and therefore cannot be assessed by the interior Fourier analysis alone. We next consider the algebraic structure of the complete system. For every interior node, the row of the global matrix has diagonal coefficient $1 + C_s + 2D_s + G_s > 0$ and off-diagonal coefficients $-(C_s + D_s) \leq 0, \quad -D_s \leq 0$. Furthermore, $1 + C_s + 2D_s + G_s - [(C_s + D_s) + D_s] = 1 + G_s > 0$. Thus every interior row is strictly diagonally dominant.

The discrete stage-coupling conditions in Section 5.2 are imposed as flux balances rather than as equality of population densities. After collecting the terms associated with the terminal node of stage

Licensed Under Creative Commons Attribution (CC BY-NC)

s and the initial node of stage $s+1$, the interface equations retain the conservative sign structure of the continuous flux formulation. In particular, the coefficients multiplying neighbouring unknowns are non-positive after the interface equations are written in the same orientation as the interior equations. Hence, provided the resulting interface rows satisfy the corresponding diagonal-dominance conditions, the complete global matrix A is a Z-matrix.

For the present fully implicit discretization, the diagonal contribution from the identity operator also remains strictly positive. Therefore, if the interface and reproductive boundary rows satisfy the same M-matrix conditions, the global matrix is a nonsingular M-matrix. In particular, $A^{-1} \geq 0$. Let the numerical solution at time level $j+1$ be given by $\mathbf{n}^{j+1} = A^{-1}\mathbf{n}^j$.
If $\mathbf{n}^j \geq 0$, then $\mathbf{n}^{j+1} = A^{-1}\mathbf{n}^j \geq 0$. Thus the numerical scheme preserves non-negativity. To establish monotonicity, consider two numerical solutions $\mathbf{n}^j$ and $\mathbf{m}^j$ satisfying the same non-negative boundary data. Their difference satisfies $A(\mathbf{m}^{j+1} - \mathbf{n}^{j+1}) = \mathbf{m}^j - \mathbf{n}^j$. If $\mathbf{m}^j - \mathbf{n}^j \geq 0$, then, because $A^{-1} \geq 0$, $\mathbf{m}^{j+1} - \mathbf{n}^{j+1} = A^{-1}(\mathbf{m}^j - \mathbf{n}^j) \geq 0$. Therefore, $\mathbf{n}^j \leq \mathbf{m}^j \implies \mathbf{n}^{j+1} \leq \mathbf{m}^{j+1}$, and the scheme is monotone. □

Thus, the interior scheme is unconditionally stable, while positivity and monotonicity of the complete stage-coupled scheme follow from the M-matrix property of the global coefficient matrix, including the interface and reproductive boundary rows.
Unlike an explicit upwind scheme, the fully implicit backward-Euler method does not impose a CFL-type restriction on Δt for stability. A smaller time step may nevertheless be required for accuracy and temporal resolution of rapidly varying solutions. Similarly, the condition $\frac{v_s \Delta a}{b_s^2} \ll 1$ is imposed to control numerical diffusion and should be interpreted as a spatial resolution condition rather than a stability restriction.
Finally, the consistency of the method follows from the truncation error $\mathcal{O}(\Delta t + \Delta a)$ of the combined time and spatial discretization. Under the regularity assumptions required for the finite-difference approximation and the stability and positivity conditions stated above, the numerical solution converges to the corresponding weak solution of the stage-coupled KFE as $\Delta t, \Delta a \to 0$. The expected global discretization error is therefore $O(\Delta t + \Delta a)$, provided that the solution has sufficient regularity.

6 Application to Fall Armyworm Population Dynamics

6.1 Non-Dimensionalization and Scaling Analysis

To analyze the relative dominance of developmental advection, variance accumulation, and mortality across stage transitions, we introduce characteristic scales for physiological age, time, and population density. Let T_0 denote the baseline lifetime duration at a reference temperature $T_{\text{ref}} = 25°\text{C}$, Δ_0 denote a characteristic stage threshold scale, and N_0 denote initial egg density [1, 2].

We define dimensionless variables (denoted by tildes) as:

$$\tilde{a} = \frac{a}{\Delta_0}, \quad \tilde{t} = \frac{t}{T_0}, \quad \tilde{n}_s = \frac{n_s \Delta_0}{N_0}.$$

Licensed Under Creative Commons Attribution (CC BY-NC)

Substituting these scaling relations into the stage-coupled KFE yields the dimensionless advection-diffusion-reaction equation [1, 2]:

$$\frac{\partial \tilde{n}_s}{\partial \tilde{t}} + \tilde{v}_s \frac{\partial \tilde{n}_s}{\partial \tilde{a}} = \frac{1}{2Pe_s} \frac{\partial^2 \tilde{n}_s}{\partial \tilde{a}^2} - \tilde{\mu}_s \tilde{n}_s, \tag{24}$$

where the dimensionless parameter groups are defined by [1, 2]:

$$\begin{aligned} \tilde{v}_s &= \frac{v_s T_0}{\Delta_0} \quad \text{(Dimensionless Development Velocity)}, \\ Pe_s &= \frac{v_s \Delta_0}{b_s^2} = \frac{u_s}{\sigma_s^2\, u_s} \quad \text{(Stage Peclet Number)}, \\ \tilde{\mu}_s &= \mu_s T_0 \quad \text{(Dimensionless Mortality Rate)}. \end{aligned}$$

The Stage Peclet number $Pe_s = \frac{u_s^2}{\sigma_s^2}$ quantifies the ratio of stage completion transport (advection) to developmental variance growth (diffusion) [1, 2]. A large Peclet number ($Pe_s \gg 1$) indicates sharp cohort synchronization, whereas $Pe_s = \mathcal{O}(1)$ reflects significant stage overlap driven by individual variability [1, 2].

The dimensionless formulation separates the effects of developmental progression, developmental variability, and mortality. In particular, the stage Peclet number measures the relative importance of advective development to diffusive developmental variability, while the dimensionless mortality rate measures demographic loss relative to the time scale.

6.2 Model Application Framework

To illustrate the practical utility of the proposed stage-coupled Kolmogorov Forward Equation (KFE) framework, the model was applied to the population dynamics of (*Spodoptera frugiperda*), a globally important agricultural pest whose development is characterized by substantial variability among individuals, overlapping generations, and strong environmental dependence [1, 2, 11]. FAW has become one of the most economically important invasive pests worldwide. It causes significant losses in maize production and poses major challenges for agricultural management, particularly in sub-Saharan Africa [4, 5].

The application is intended to demonstrate the practical implementation of the mathematical framework developed rather than to perform empirical parameter estimation or field validation. We illustrate how a continuous physiological-age formulation can be used to represent developmental progression, developmental variability, mortality, and stage transitions within a biological population.

Representative developmental characteristics for the stages of Fall Armyworm were specified using the developmental means and variances employed in the simulations. The corresponding KFE parameters were then obtained directly from the moment-based parametrization derived in Section 4. This ensures that the KFE coefficients are linked to observable developmental characteristics rather than being independently selected. For comparison with the DDM, the same developmental means and variances

Licensed Under Creative Commons Attribution (CC BY-NC)

were used to parameterize the corresponding compartmental model. Thus, the two formulations are compared using equivalent developmental statistics while retaining their distinct representations of developmental variability.

6.3 Simulation Parameter Set-up

Table 1: Parameter values used in simulation

Stage	Δ_s	μ_s	v_s	b_s^2	k_s
Eggs	1.0	0.1	1.0	0.1	10
Larvae	5.0	0.06	1.0	0.1	10
Pupae	7.0	0.05	1.0	0.1	10
Adults	29.0	0.03	1.0	0.1	10

Table 1 summarizes the developmental parameters used in the simulations. The KFE coefficients v_s and b_s^2 were obtained from the developmental mean u_s and variance σ_s^2 using the moment-based parametrization derived in Section 4.

6.4 Continuous Physiological-Age Dynamics and Cohort Progression

Licensed Under Creative Commons Attribution (CC BY-NC)

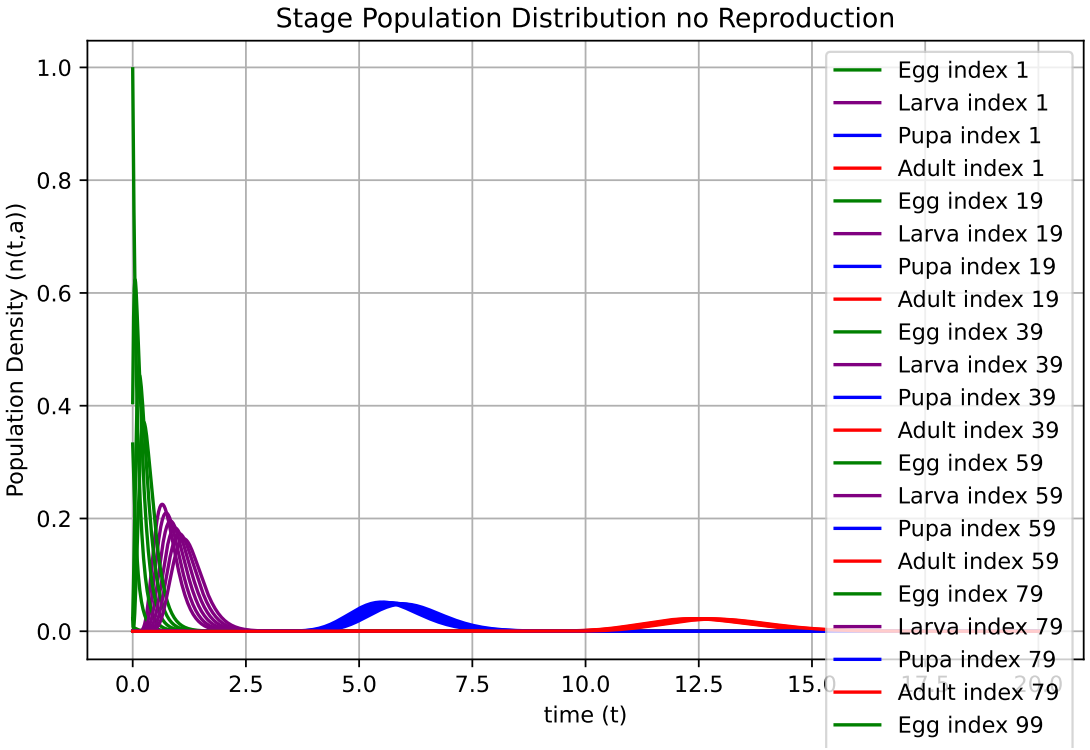

Figure 1: Evolution of physiological-age distributions within successive Fall Armyworm developmental stages at selected numerical time steps. The indices 1, 19, 39, ... denote the corresponding time-step indices selected to illustrate the progression of the population.

The primary advantage of the KFE formulation is its ability to represent developmental progression continuously across physiological age. Figure 1 illustrates the evolution of stage-specific population densities at several representative time points. As development proceeds, the population density profile within each stage translates towards larger physiological ages while simultaneously becoming increasingly dispersed.

The observed displacement is governed by the advection component of the KFE and reflects deterministic developmental progression through physiological age. In contrast, the widening of the profile is generated by the diffusion term and represents developmental variability among individuals. Even when individuals experience identical environmental conditions, variation in physiological processes, genetic characteristics, and micro-environmental influences can lead to substantial differences in developmental timing. The diffusion term captures this phenomenon directly within the governing equation. An important result of this representation is the emergence of naturally overlapping developmental stages. Unlike deterministic models, where individuals advance simultaneously through development, the KFE framework predicts that some individuals complete development earlier while others remain within

Licensed Under Creative Commons Attribution (CC BY-NC)

the same stage for a longer periods. This results in broad physiological-age distributions and gradual transitions between successive life stages.

The continuous physiological-age formulation therefore eliminates the need for artificial compartmental structures traditionally employed in distributed delay models. Developmental heterogeneity emerges directly from the underlying stochastic dynamics rather than from the choice of compartment number. This provides a biologically meaningful interpretation of developmental variability while simultaneously preserving mathematical consistency with the underlying physiological-age process.

Furthermore, the smooth progression observed in Figure 1 demonstrates that the KFE framework avoids the abrupt stage-transition artifacts that can arise in highly discretised developmental models. The resulting trajectories provide a more realistic representation of insect population development and establish a direct connection between individual-level developmental variability and population-level dynamics.

6.5 Population Dynamics and Generational Turnover

While physiological-age distributions provide insight into developmental mechanisms, practical applications often require analysis of total population abundance within each life stage. Aggregating the physiological-age densities across each developmental interval yields stage-specific population trajectories.

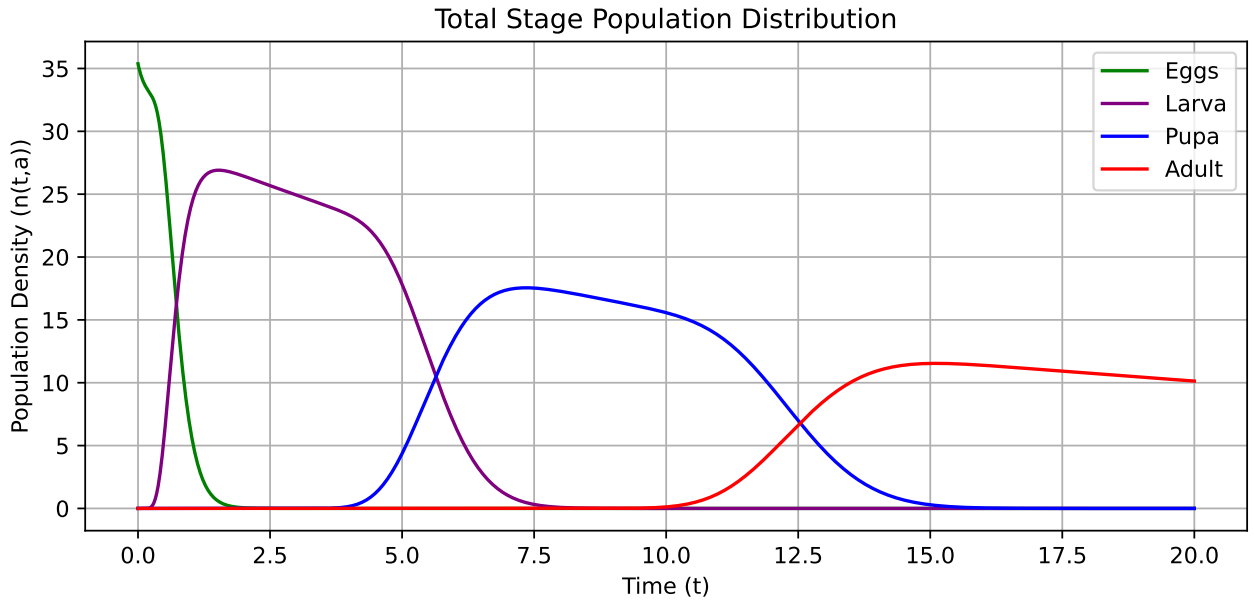

Figure 2: Population trajectories generated by the stage-coupled KFE framework in the absence of reproduction.

Figure 2 illustrates population dynamics when reproduction is excluded from the model. In this scenario, population abundance declines progressively as individuals experience transition through

Licensed Under Creative Commons Attribution (CC BY-NC)

successive developmental stages. The gradual reduction in abundance reflects the cumulative effects of mortality acting throughout the life cycle. Timing of developmental transitions remains strongly influenced by the underlying physiological-age dynamics. The smooth movement of population mass between successive stages demonstrates the ability of the KFE framework to preserve developmental continuity while maintaining biologically realistic stage transitions.

When reproduction is incorporated, the population dynamics become considerably more complex due to feedback generated by oviposition and recruitment into the egg stage. The resulting system exhibits recurrent generational cycles and overlapping cohorts arising from developmental variability.

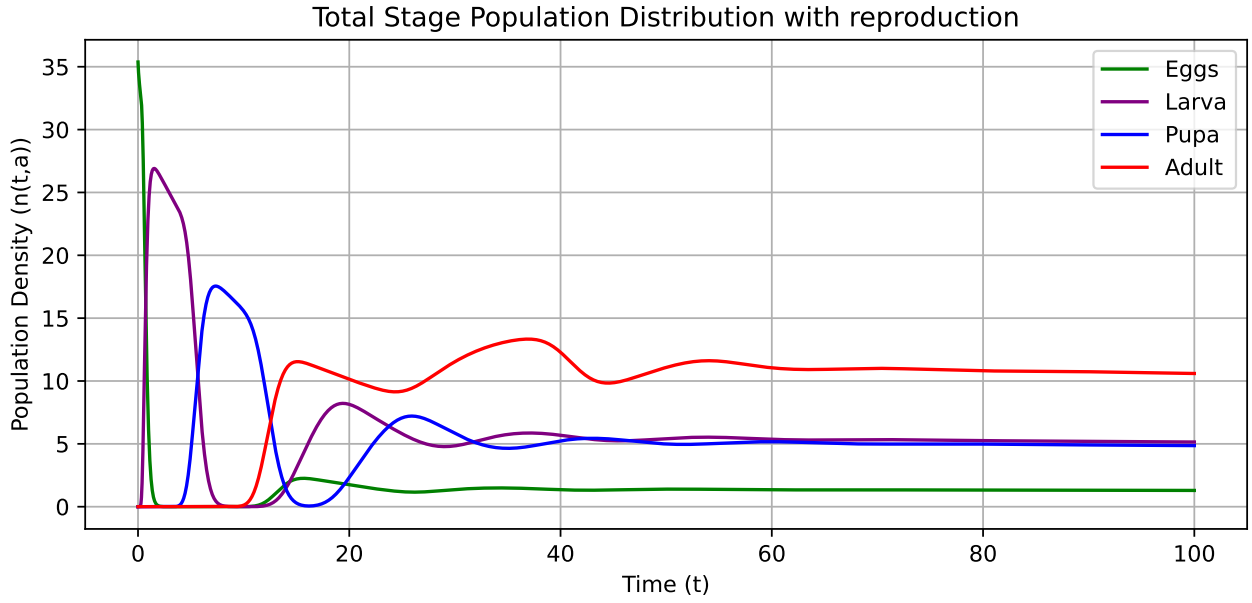

Figure 3: Population trajectories generated by the stage-coupled KFE framework with adult reproduction.

As shown in Figure 3, reproductive feedback generates recurrent population cycles corresponding to successive generations. Following adult emergence, oviposition produces a new cohort of eggs that subsequently progresses through the developmental sequence. The interaction between reproduction, mortality, and developmental variability generates oscillatory population dynamics characterized by overlapping generations. Importantly is the absence of sharply separated generational cohorts in the simulations. This behavior emerges naturally from developmental variability and reflects observations commonly reported in field populations of Fall Armyworm, where multiple developmental stages are frequently present simultaneously.

For the stage-structured population, the basic reproduction number R_0 is defined as the expected number of offspring produced by a typical individual over its lifetime in a population. In the present framework, R_0 depends on survival through the developmental stages, developmental completion times,

Licensed Under Creative Commons Attribution (CC BY-NC)

and the reproduction rate of the adult stage. Thus, $R_0 > 1$ indicates potential population growth, whereas $R_0 < 1$ indicates population decline.

6.6 Sensitivity of Developmental Dynamics to Model Parameters

Understanding how model parameters influence developmental dynamics is essential for both biological interpretation and practical application. Sensitivity analyses were therefore performed with respect to developmental velocity, diffusion intensity, and mortality rate.

6.6.1 Effect of Developmental Velocity

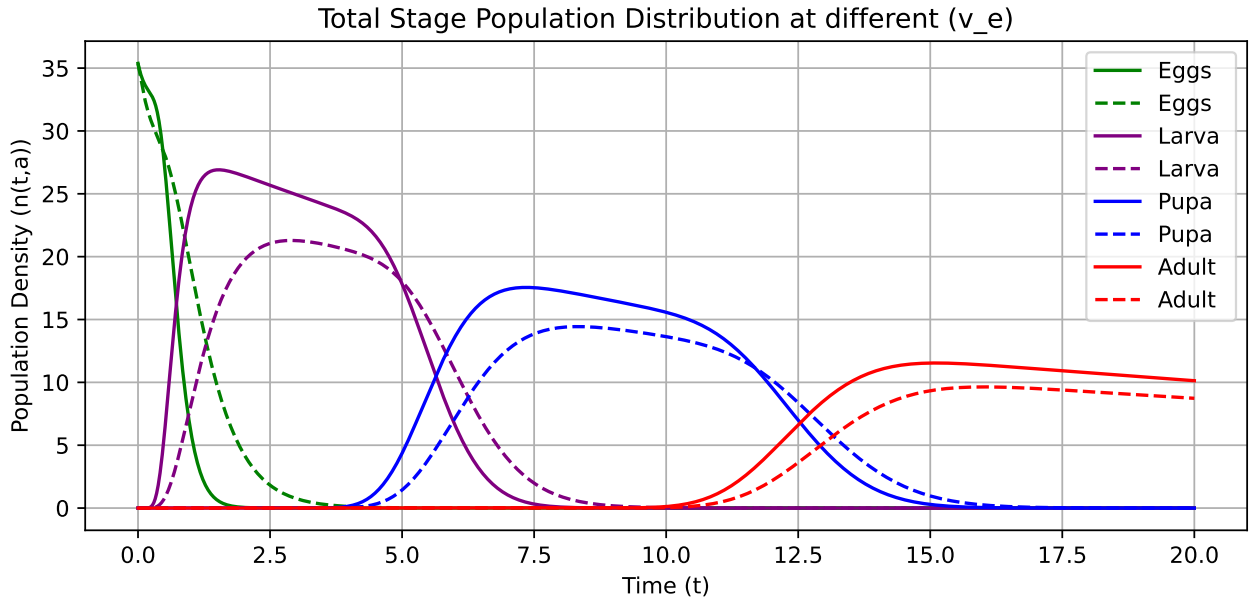

Figure 4: Sensitivity of population dynamics to developmental velocity. The solid curve represents $v_e = 1.0$, while the dashed curve represents $v_e = 0.5$.

Figure 4 shows that increasing developmental velocity accelerates physiological-age progression and leads to earlier completion of development. Consequently, subsequent life stages appear sooner and generational turnover occurs more rapidly. Conversely, reduced developmental velocity delays developmental completion and extends generation times. From a biological perspective, developmental velocity is closely associated with environmental conditions such as temperature. The results therefore suggest that environmental variation can substantially influence the timing of Fall Armyworm population outbreaks by altering developmental progression rates.

6.6.2 Effect of Developmental Variability

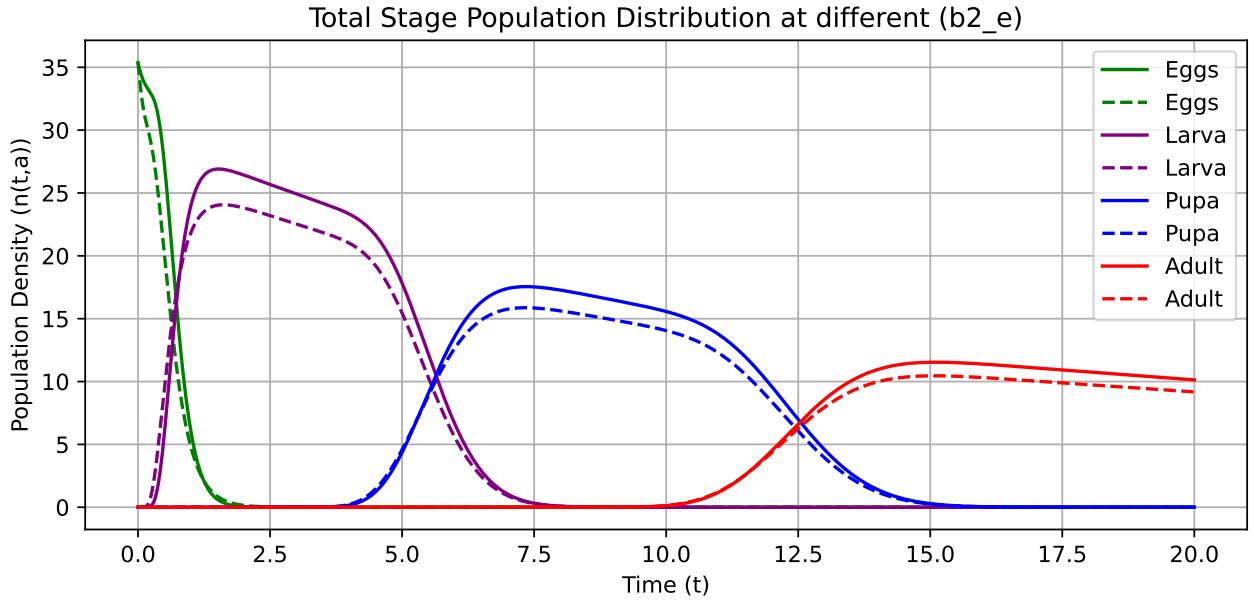

Figure 5: Sensitivity of population dynamics to diffusion. The solid curve represents $b_e^2 = 0.1$, while the dashed curve represents $b_e^2 = 0.2$.

The diffusion coefficient controls the magnitude of developmental variability within the population. As shown in Figure 5, increasing diffusion intensity produces broader physiological-age distributions and greater overlap among developmental stages. Population peaks become less pronounced and developmental transitions occur over longer periods. This result highlights the importance of developmental heterogeneity in determining outbreak duration. Greater variability implies that damaging larval stages remain present in the population over an extended time interval, potentially complicating pest management interventions that rely on accurate timing of control measures.

Licensed Under Creative Commons Attribution (CC BY-NC)

6.6.3 Effect of Mortality

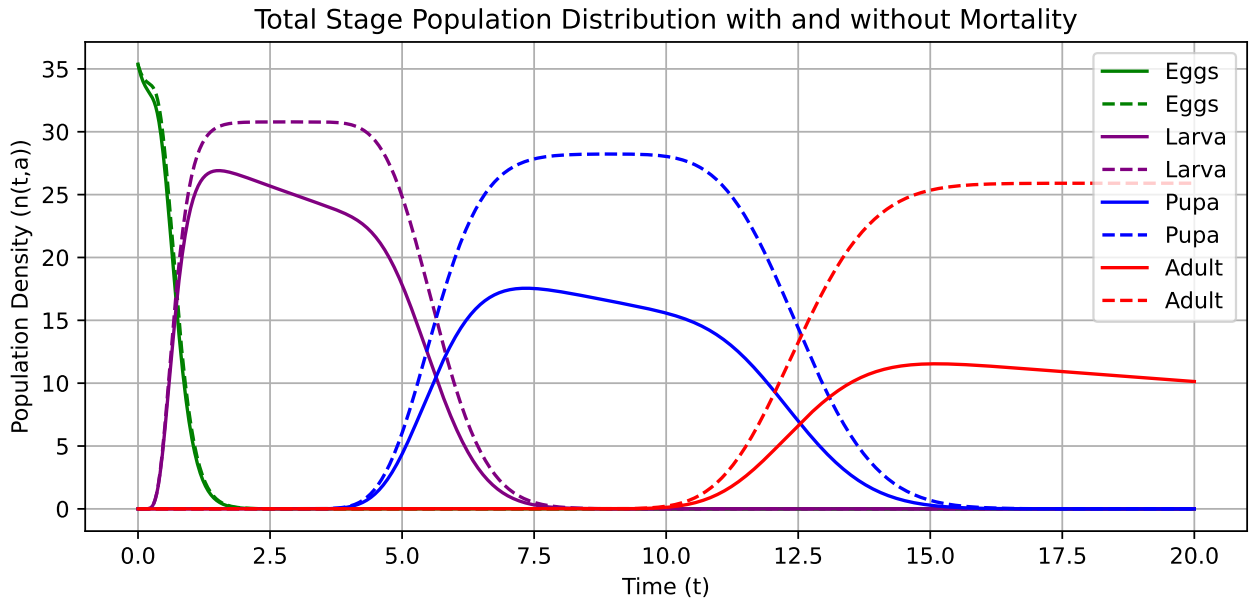

Figure 6: Sensitivity of population dynamics to mortality. The solid curve represents stage mortalities, while the dashed curve no mortality.

Figure 6 demonstrates that mortality primarily influences population magnitude rather than developmental timing. Increasing mortality suppresses population abundance across all developmental stages while leaving the overall structure of developmental progression largely unchanged.

Collectively, the sensitivity analyses reveal distinct biological roles for the model parameters. Developmental velocity governs the timing of developmental progression, diffusion determines developmental heterogeneity and stage overlap, while mortality regulates population abundance and outbreak intensity.

6.7 Comparison with Distributed Delay Models

The numerical simulations compare the DDM and stage-coupled KFE using equivalent developmental parameters.

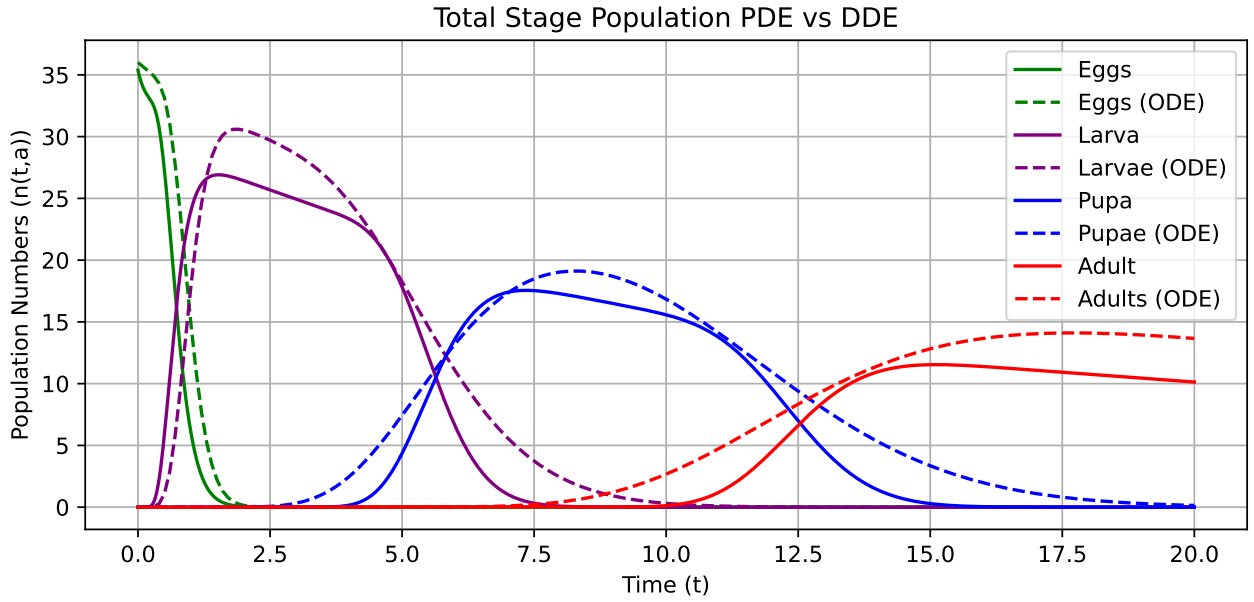

Figure 7: Comparison of population trajectories generated by the Distributed Delay Model and the stage-coupled Kolmogorov Forward Equation framework using equivalent developmental parameters.

Figure 7 shows broadly comparable population dynamics in the two formulations, including developmental timing, stage transitions, and population peaks. The DDM produces sharper transitions due to its finite compartmental representation, whereas the KFE produces smoother trajectories because physiological age is represented continuously and developmental variability is controlled through the diffusion coefficient.

The observed differences therefore arise from the distinct representations of developmental variability in the two models, despite their use of equivalent developmental parameters.
The effects of developmental velocity, diffusion, and mortality are not necessarily independent. For example, increased developmental velocity may reduce the time individuals are exposed to mortality, while increased developmental variability may increase the proportion of individuals experiencing longer developmental durations and therefore greater cumulative mortality. Hence, interactions among these parameters can influence both the magnitude and timing of population peaks. A systematic analysis of these interactions provides a useful direction for future work.

6.8 Implications for Physiologically Structured Population Modeling

The Fall Armyworm application demonstrates that the stage-coupled KFE framework extends beyond existing distributed delay models. By representing physiological age as a continuous stochastic variable, the framework provides a mechanistic description of developmental variability while maintaining direct connections to biologically measurable developmental statistics.
The framework achieves three important objectives simultaneously. First, it preserves consistency with

Licensed Under Creative Commons Attribution (CC BY-NC)

established distributed delay methodologies through the moment-based parametrization developed in Section 4. Second, it provides a biologically interpretable representation of developmental variability through explicit diffusion processes. Third, it supports efficient numerical implementation through positivity-preserving finite difference schemes that maintain stability and biological realism. These suggest that the stage-coupled KFE framework provides a unified mathematical foundation for physiologically structured population models. Although demonstrated here using Fall Armyworm, the framework is sufficiently general to accommodate a wide range of organisms exhibiting developmental variability and stage-structured life cycles.

The results therefore support the central claim of this study that continuous physiological-age formulations based on Kolmogorov Forward Equations provide a mathematically rigorous and biologically interpretable alternative to traditional compartmental distributed delay models while preserving consistency with established developmental theory.

7 Discussion

The results show that the KFE provides a continuous representation of developmental variability, with developmental velocity controlling the timing of progression and diffusion controlling the spread of developmental times. The Fall Armyworm application illustrates how this representation allows developmental heterogeneity to be incorporated directly into a stage-structured population model.

A limitation of the present formulation is the assumption of time-independent developmental parameters and homogeneous environmental conditions. In biological applications, developmental rates may vary with temperature and other environmental factors. Future work should therefore incorporate temperature-dependent developmental parameters, environmental forcing, spatial dispersal, and parameter estimation from experimental data.

8 Conclusions

The framework developed here extends the original formulation by introducing physiological-age boundary fluxes that connect successive developmental stages. This extension allows the representation of complete life cycles while preserving the stochastic interpretation of developmental variability. Deterministic progression, developmental heterogeneity, mortality, and stage transitions are therefore incorporated within a single mathematically consistent framework. Importantly, the proposed formulation is not restricted to a particular species. Rather, it provides a general modeling framework applicable to a broad class of stage-structured populations, including insects, aquatic organisms, and other species whose development proceeds through discrete biological stages.

Applied to Fall Armyworm population dynamics, the numerical results demonstrated the effects of developmental velocity, diffusion, and mortality on stage progression and population dynamics. Comparison with distributed delay models showed comparable overall developmental behaviour. The framework therefore provides a basis for further modeling of stage-structured populations under environmentally varying conditions.

Licensed Under Creative Commons Attribution (CC BY-NC)

References

[1] C. S. Barfield, E. Mitchell, and S. Poeb. A temperature-dependent model for fall armyworm development. *Annals of the Entomological Society of America*, 71(1):70–74, 1978.

[2] F. Baudron, M. A. Zaman-Allah, I. Chaipa, N. Chari, and P. Chinwada. Understanding the factors influencing fall armyworm (spodoptera frugiperda je smith) damage in african smallholder maize fields and quantifying its impact on yield. a case study in eastern zimbabwe. *Crop protection*, 120:141–150, 2019.

[3] V. Bellagamba, G. Di Cola, and R. Cavalloro. Stochastic models in fruit-fly population dynamics. In *Proceedings of the CEE/IOBC International Symposium*, pages 91–98, 1987.

[4] M. J. Cock, P. K. Beseh, A. G. Buddie, G. Cafá, and J. Crozier. Molecular methods to detect spodoptera frugiperda in ghana, and implications for monitoring the spread of invasive species in developing countries. *Scientific reports*, 7(1):4103, 2017.

[5] R. Day, P. Abrahams, M. Bateman, T. Beale, V. Clottey, M. Cock, Y. Colmenarez, N. Corniani, R. Early, J. Godwin, et al. Fall armyworm: impacts and implications for africa. *Outlooks on pest management*, 28(5):196–201, 2017.

[6] G. Di Cola, G. Gilioli, and J. Baumgärtner. Mathematical models for age-structured population dynamics: an overview. *Population and Community Ecology for Insect Management and Conservation*, pages 45–62, 2020.

[7] A. P. Gutierrez. *Applied population ecology: a supply-demand approach*. John Wiley & Sons, 1996.

[8] T. J. Manetsch. Time-varying distributed delays and their use in aggregative models of large systems. *IEEE Transactions on Systems, Man, and Cybernetics*, 6:547–553, 1976.

[9] M. A. Mirhosseini, Y. Fathipour, and G. V. Reddy. Arthropod development's response to temperature: a review and new software for modeling. *Annals of the Entomological Society of America*, 110(6):507–520, 2017.

[10] B. Oksendal. *Stochastic differential equations: an introduction with applications*. Springer Science & Business Media, 2013.

[11] K. Overton, J. L. Maino, R. Day, P. A. Umina, B. Bett, D. Carnovale, S. Ekesi, R. Meagher, and O. L. Reynolds. Global crop impacts, yield losses and action thresholds for fall armyworm (spodoptera frugiperda): A review. *Crop Protection*, 145:105641, 2021.

[12] J. Régnière, J. Powell, B. Bentz, and V. Nealis. Effects of temperature on development, survival and reproduction of insects: experimental design, data analysis and modeling. *Journal of insect physiology*, 58(5):634–647, 2012.

[13] W. Suwansantisuk, M. Z. Win, and L. A. Shepp. First passage time problems with applications to synchronization. In *2012 IEEE International Conference on Communications (ICC)*, pages 2580–2584. IEEE, 2012.

[14] M. C. Tweedie. Statistical properties of inverse gaussian distributions. i. *The Annals of Mathematical Statistics*, 28(2):362–377, 1957.

[15] J. VanSickle. Analysis of a distributed-parameter population model based on physiological age. *Journal of theoretical Biology*, 64(3):571–586, 1977.

©*Onyango et al. 2026.; This is an Open Access article distributed under the terms of the Creative Commons Attribution License http://creativecommons.org/licenses/by/4.0, which permits unrestricted use, distribution, and reproduction in any medium, provided the original work is properly cited.*

Licensed Under Creative Commons Attribution (CC BY-NC)